Complexin II plays a positive role in Ca^{2+}-triggered exocytosis by facilitating vesicle priming

Haijiang Cai[a,1], Kerstin Reim[b], Frederique Varoqueaux[b], Sompol Tapechum[a,2], Kerstin Hill[c,3], Jakob B. Sørensen[c], Nils Brose[b], and Robert H. Chow[a,4]

[a]Department of Physiology and Biophysics, Keck School of Medicine, Zilkha Neurogenetic Institute, University of Southern California, Los Angeles, CA 90089; [b]Department of Molecular Neurobiology and Center for the Molecular Physiology of the Brain, Max Planck Institute of Experimental Medicine, D-37075 Göttingen, Germany; and [c]Department of Membrane Biophysics, Max Planck Institute for Biophysical Chemistry, D-37077 Göttingen, Germany

Communicated by Clay M. Armstrong, University of Pennsylvania, Philadelphia, PA, October 10, 2008 (received for review August 3, 2008)

SNARE-mediated exocytosis is a multistage process central to synaptic transmission and hormone release. Complexins (CPXs) are small proteins that bind very rapidly and with a high affinity to the SNARE core complex, where they have been proposed recently to inhibit exocytosis by clamping the complex and inhibiting membrane fusion. However, several other studies also suggest that CPXs are positive regulators of neurotransmitter release. Thus, whether CPXs are positive or negative regulators of exocytosis is not known, much less the stage in the vesicle life cycle at which they function. Here, we systematically dissect the vesicle stages leading up to exocytosis using a knockout-rescue strategy in a mammalian model system. We show that adrenal chromaffin cells from CPX II knockout mice exhibit markedly diminished releasable vesicle pools (comprising the readily and slowly releasable pools), while showing no change in the kinetics of fusion pore dilation or morphological vesicle docking. Overexpression of WT CPX II—but not of SNARE-binding-deficient mutants—restores the size of the the releasable pools in knockout cells, and in WT cells it markedly enlarges them. Our results show that CPXs regulate the size of the primed vesicle pools and have a positive role in Ca^{2+}-triggered exocytosis.

chromaffin cell | large dense core vesicle | SNARE complex

Properly regulated exocytosis is important for the release of neurotransmitters and hormones from membrane-delimited vesicles. Secretory vesicles must dock at the plasma membrane and then undergo priming or maturation to become "readily releasable"—that is, competent to fuse rapidly with the plasma membrane in response to a Ca^{2+} trigger. It is generally accepted that exocytosis is mediated by SNARE proteins, whose function is fine tuned through interaction with other proteins (1). Three SNARE proteins comprise the minimal machinery underlying vesicle fusion: one vesicle membrane protein synaptobrevin (also called VAMP: vesicle-associated membrane protein) and the two plasma membrane proteins, syntaxin and SNAP-25 (2–4). These 3 proteins form a stable 4-helical bundle called the SNARE core complex that drives intracellular membrane fusion. Although *in vitro* studies have shown that these 3 SNARE proteins alone suffice to fuse the membranes of artificial liposomes, the rate of such fusions is orders of magnitude slower than fusion in regulated exocytosis, which takes place on a millisecond time scale (5, 6), indicating that additional factors are involved in fast regulated secretion.

Complexin (CPX) is a small neuronal protein that binds very rapidly ($\approx 5 \times 10^7 M^{-1} \cdot s^{-1}$) and with a 1:1 stoichiometry and high affinity to the SNARE core complex (7–12), which is indicative of a regulatory role in fast exocytosis. Four CPX isoforms have been identified in vertebrates, CPX I - IV (13). They all are enriched particularly in the nervous system, where they exhibit a differential distribution, but some CPXs are also found in other tissues (7, 13). The function of CPXs in regulated exocytosis is still a matter of controversy. Several early studies indicated that CPXs play a negative role in regulated exocytosis. Injection of recombinant CPX II caused depression of release, presynaptic injection of anti-CPX II antibody into *Aplysia buccal* ganglia neurons stimulated neurotransmitter release (14), and overexpression of CPX I or CPX II in PC12 cells was reported to suppress acetylcholine (ACh) release (15). More recent studies showed that cell–cell fusion of cells that express SNAREs facing extracellularly is inhibited by CPX (16–18) and that overexpression of a synaptobrevin CPX fusion protein, which is thought to cause high presynaptic levels of CPX, inhibits synaptic transmission (19). The inhibitory role of CPX was further supported by the result that spontaneous release was increased in the *Drosophila* neuromuscular junction where CPX was knocked out (20). In addition, data on bovine chromaffin cells overexpressing CPX II were interpreted to indicate a role of CPXs in the regulation of fusion pore dynamics (21). Taken together, these data led to the notion that CPXs play an inhibitory role in fusion by clamping SNARE complexes.

Other studies, however, indicate that CPXs play a positive role in regulated exocytosis. In pancreatic β-cells, insulin secretion is enhanced by overexpressing CPX I, and decreased by silencing CPX I expression with RNA interference (22). In mast cells, a knockdown of CPX II also led to suppressed secretion (23). CPX I/II double knockout neurons displayed dramatically reduced neurotransmission, associated with a change in the apparent Ca^{2+} sensitivity of exocytosis (24). And distinct domains of CPX are recently proposed to have different functions (25). Thus, the role of CPX remains to be clarified (26).

For the present study, we used mouse adrenal chromaffin cells, a well-characterized and extensively used model system for studying Ca^{2+}-triggered exocytosis, and applied several methods to dissect out the role of CPXs in the stages of regulated exocytosis from vesicle docking to fusion pore formation. Our data demonstrate that CPX II has a positive role in fast vesicle exocytosis by regulating the size of the primed vesicle pools.

Results

CPX Isoform Expression. Chromaffin cells secrete catecholamine through the fusion of large dense core vesicles (LDCVs) with the plasma membrane, employing the same conserved SNARE-based fusion machinery that also mediates synaptic transmitter release

Author contributions: H.C., J.B.S., N.B., and R.H.C. designed research; H.C., K.R., F.V., S.T., K.H., and J.B.S. performed research; K.R. and S.T. contributed new reagents/analytic tools; H.C., K.R., F.V., K.H., and J.B.S. analyzed data; and H.C., J.B.S., N.B., and R.H.C. wrote the paper.

The authors declare no conflict of interest.

[1]Present address: Division of Biology 216-76, California Institute of Technology, Pasadena, CA 91125.

[2]Present address: Department of Physiology, Faculty of Medicine Siriraj Hospital, Mahidol University, Bangkok 10700, Thailand.

[3]Present address: Rudolf-Boehm-Institut für Pharmakologie und Toxikologie, Universität Leipzig, Härtelstrasse 16-18, 04107 Leipzig, Germany.

[4]To whom correspondence should be addressed. E-mail: rchow@usc.edu.

This article contains supporting information online at www.pnas.org/cgi/content/full/0810232105/DCSupplemental.

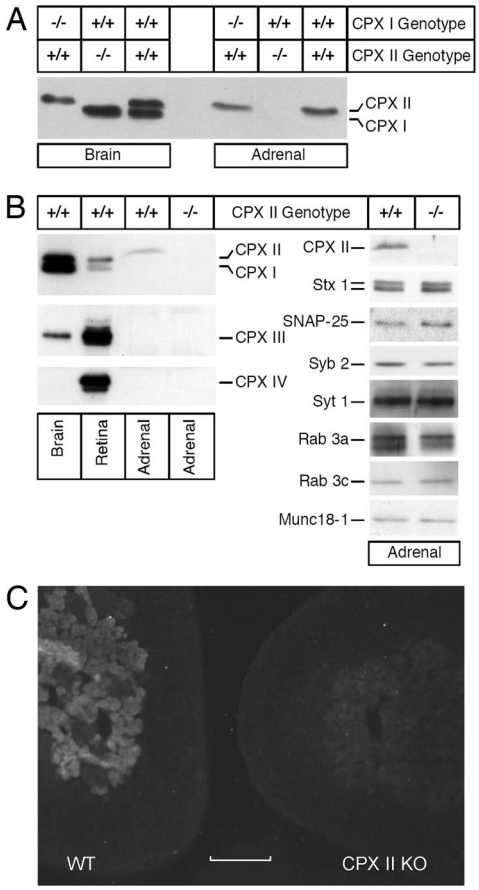

Fig. 1. CPXs expression. (*A*) Western blot analyses of CPX I and CPX II expression levels in homogenates of brain (5 μg per lane) and adrenal gland (50 μg per lane) from mice of the indicated CPX I and CPX II genotypes. (*B*) (*Left*) Western blot analyses of CPX expression levels in homogenates of brain (5 μg per lane) and adrenal gland (50 μg per lane) from mice of the indicated CPX II genotypes. (*Right*) Western blot analyses of the expression levels of CPX II and selected presynaptic proteins in adrenal gland homogenates [50 μg per lane, except for SNAP-25 and Syntaxin 1 (10 μg per lane) and Synaptotagmin 1 (25 μg per lane)] from mice of the indicated CPX II genotypes. Analyses were conducted on 3 mice for each of the indicated CPX II genotypes, and the blots shown are representative. CPX, Complexin; Stx 1, Syntaxin 1; Syb 2, Synaptobrevin 2; Syt 1, Synaptotagmin 1. (*C*) Immuno-histochemical staining of cryostat sections from WT (*Left*) and CPX II$^{-/-}$ (*Right*) mice with antibodies against CPX I/II. Only the medulla chromaffin cells from the WT animals show bright CPX labeling. (Scale bar: 100 μm.)

from neurons. Because there are 4 CPX isoforms in vertebrates, CPX I-IV (13), an important advantage of chromaffin cells is that they express only one major CPX isoform, CPX II, and knockout of CPX II does not up-regulate the expression of other CPX isoforms or alter the expression level of other presynaptic proteins (Fig. 1).

When we started colonies (24) with heterozygous CPX II$^{+/-}$ breeding pairs, the offspring showed the expected Mendelian assortment of genotypes (33 CPX II$^{+/+}$, 60 CPX II$^{+/-}$, 30 CPX II$^{-/-}$ in 20 randomly picked litters), indicating that gestation was not terminated prematurely in CPX II$^{-/-}$ or CPX II$^{+/-}$ embryos. CPX II$^{-/-}$ mice appeared normal when young and were able to reproduce. The cultured chromaffin cells of CPX II$^{-/-}$ and CPX II$^{+/+}$ animals showed no morphological difference and had similar cell size, as measured by basal membrane capacitance (4.82 $\pm$ 0.13 pF, n = 29 CPX II$^{+/+}$ cells; 5.02 $\pm$ 0.18 pF, n = 30 CPX II$^{-/-}$ cells).

Single Amperometric Event Characteristics in CPX II$^{-/-}$ Cells. Because CPXs bind to the assembled SNARE core complex (7), and SNARE proteins are known to play a role in the behavior of the fusion pore (27–30)—the aqueous pore that initially connects the vesicle lumen and extracellular space during exocytosis—we tested whether the kinetics of fusion pore dilation is altered in the CPX II$^{-/-}$ chromaffin cells. We used amperometry, an electrochemical technique that directly reports the kinetics and amount of catecholamine release from individual vesicles. Our results show that, for all of the parameters examined, there is no robust difference between CPX II$^{-/-}$ and CPX II$^{+/+}$ mouse chromaffin cells (Fig. 2), indicating that CPX does not affect the fusion pore formation and dilation step of Ca^{2+}-triggered exocytosis, or its effect is very subtle.

Secretion Triggered by Trains of Depolarizations. To examine whether other secretory steps are compromised in CPX II$^{-/-}$ chromaffin cells, we next applied the method of membrane capacitance measurement, an approach for monitoring changes in the membrane surface area of the entire plasma membrane at millisecond time resolution. We applied a train of 8 100-ms depolarizations separated by 100-ms intervals (Fig. 3*A*), and recorded the capacitance increase (ΔC_m) (Fig. 3*C*), to obtain a measure of the secretion capacity and dynamics. Although the total Ca^{2+} influx was the same for CPX II$^{-/-}$ and CPX II$^{+/+}$ cells (Fig. 3 *B* and *F*), the total capacitance increase was significantly smaller in CPX II$^{-/-}$ cells (Fig. 3 *C* and *G*). The most significant differences in ΔC_m occurred during the earlier depolarizations, whereas the ΔC_m in response to later depolarizations, especially to the 7th and 8th depolarizations, were indistinguishable (Fig. 3*E*). The selective reduction in the response to the earlier depolarizations of the train is consistent with a function of CPX II in rendering vesicles release-ready, thereby increasing the size of the releasable vesicle pools.

Secretion Triggered by Flash Photolysis of Caged Ca^{2+}. The most direct approach to measure the size of the functional vesicle pools in chromaffin cells is to monitor the ΔC_m in response to a uniform and global step elevation of the cytosolic Ca^{2+} concentration ($[Ca^{2+}]_i$), achieved by photolysis of caged Ca^{2+} compounds. The multiphasic rising C_m trace can be fitted with a triple exponential function (28), which provides quantitative information about the functional vesicle pools. The two fastest components correspond to the primed (releasable) vesicle pools, comprising the readily releasable pool (RRP) and the slowly releasable pool (SRP) (31).

We used the whole-cell patch clamp technique to load chromaffin cells with a caged Ca^{2+} compound (NP-EGTA), and monitored the capacitance change upon applying a $\approx$1 ms UV (UV) flash. Because at normal basal Ca^{2+} concentration ($\approx$500 nM), exocytosis in CPX II$^{-/-}$ cells is too small for accurate kinetic analysis [supporting information (SI) Fig. S1], we increased the basal Ca^{2+} concentration to 1–3 μM in our experiments, which has been shown to increase equally both the RRP and SRP of the exocytotic burst but not to affect the release kinetics (32). Upon flashing, the $[Ca^{2+}]_i$ was elevated to 15–20 μM (Fig. 4*A*). As expected (Fig. 4*B*), the capacitance response was multiphasic for CPX II$^{-/-}$ and CPX II$^{+/+}$ cells. However, CPX II$^{-/-}$ cells had a much-reduced exocytotic burst, whereas their sustained phase was not significantly altered (Fig. 4*B*). As seen in Fig. 4*D*, the fast and slow burst phases were both reduced in amplitude in CPX II$^{-/-}$ cells, but their time constants were unchanged (Fig. 4 *B Inset* and *E*), indicating that the kinetics of vesicle pool emptying is not affected by CPX II loss. The reduced capacitance response was confirmed to be due to reduced secretion (and not enhanced endocytosis) by simultaneous amperometry measurements of the release of oxidizable vesicle content. The time-integral of the amperometry measurements gave traces showing cumulative secretion, resembling those obtained by the capacitance method (Fig. 4*C*), however, without the potential confounding effects of overlapping endocytosis. These results confirmed that the size of the releasable vesicle pools is decreased in CPX II$^{-/-}$ cells.

PHYSIOLOGY

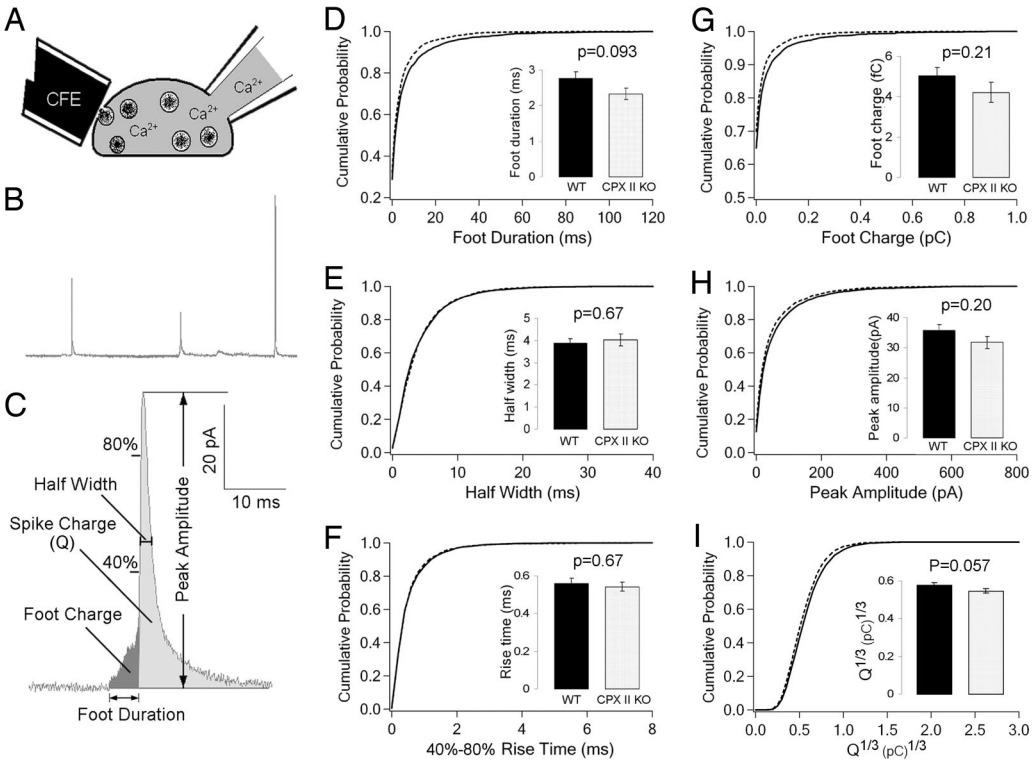

Fig. 2. Characteristics of single amperometric events. (*A*) Experimental configuration of whole-cell patch clamp combined with amperometry, carbon fiber electrode (CFE). (*B*) Sample amperometry recording. The introduction of Ca^{2+} at 10 μM via the pipette triggers exocytotic events at such a frequency that the individual amperometric spikes, representing single-vesicle exocytosis, are well-separated. (*C*) Characteristics of a single amperometric event. (*D–I*) Cumulative distribution of single amperometric event characteristics. (*Insets*) Bar graphs show the mean ± SEM of corresponding parameters. A total of 49 WT cells (n = 49) from 6 animals (solid lines, WT) and 53 CPX II$^{-/-}$ cells (n = 53) from 6 animals (dashed lines, CPX II KO) were analyzed. Spikes (12–100) were recorded from each cell.

Rescue of Secretion in CPX II$^{-/-}$ Cells by Transducing CPX II. One concern about experiments with knockout mice is that the phenotype observed may be due not only to the absence of the deleted gene, but also to secondary and irreversible changes that do not directly reflect the loss of the eliminated gene product, such as compensatory changes that occur during development. We therefore tested whether expressing CPX II in CPX II$^{-/-}$ cells would rescue the diminished secretion. We generated Semliki Forest Virus (SFV) vectors encoding either CPX II-IRES-EGFP, which allows both CPX II and EGFP (enhanced green fluorescence protein) to be expressed separately in the same cell, or IRES-EGFP only (as control). EGFP serves as a marker of the infected cells that express CPX II. The expression of CPX II and EGFP was confirmed by immunocytochemical labeling with an antibody to CPX I/II (Fig. 5*A*). Fig. 5 and Fig. S2 illustrate that expression of CPX II in the knockout background rescued the decreased release, and that the time constants of the slow and rapid burst of the capacitance increase were not changed (Fig. S2).

Enhanced Secretion in CPX II$^{+/+}$ Cells by Transducing CPX II. To investigate how overexpression of CPX II would affect secretion, we infected WT cells with the bicistronic SFV vector encoding CPX II-IRES-EGFP (WT+CPXII), and compared the results with WT

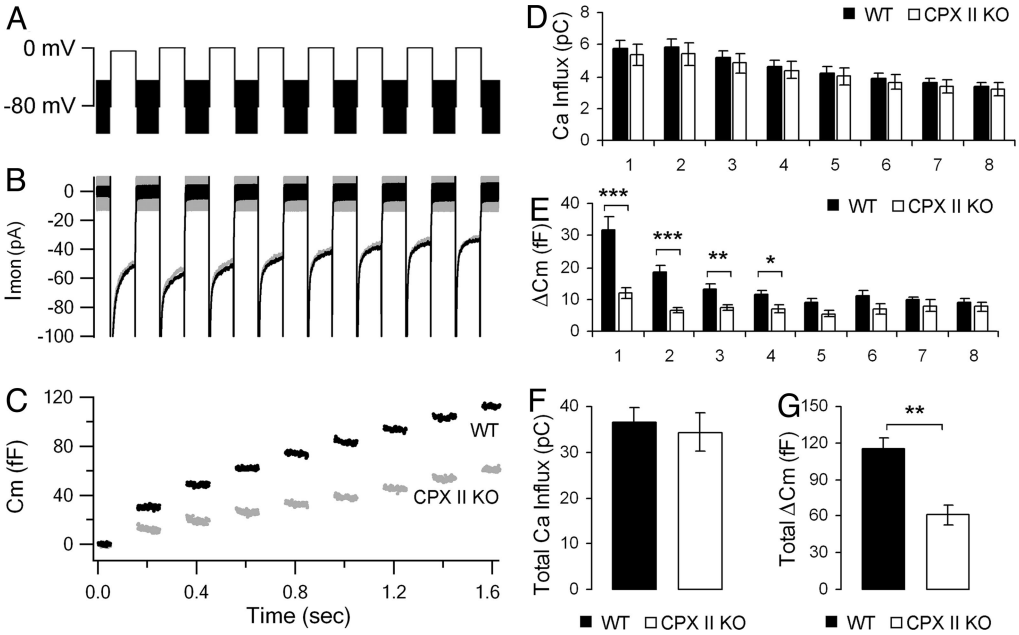

Fig. 3. Secretion triggered by trains of depolarizations. (*A*) Voltage protocol with eight 100-ms depolarizations. (*B* and *C*) Averaged ionic currents (*B*) and membrane capacitance response (*C*) from CPX II$^{-/-}$ (gray) and WT (black) cells. C_m before stimulus was subtracted. (*D–G*) Ca^{2+} influxes and ΔC_m for each of the individual 8 depolarizations (*D* and *E*) and summed over all 8 depolarizations (*F* and *G*). Data were averaged from 26 experiments from 15 WT cells, 3 animals (n = 26, black), and from 20 experiments from 15 CPX II$^{-/-}$ cells, 3 animals (n = 20, white). Data are expressed as mean ± SEM. *, $P < 0.01$; **, $P < 0.005$; ***, $P < 0.00005$.

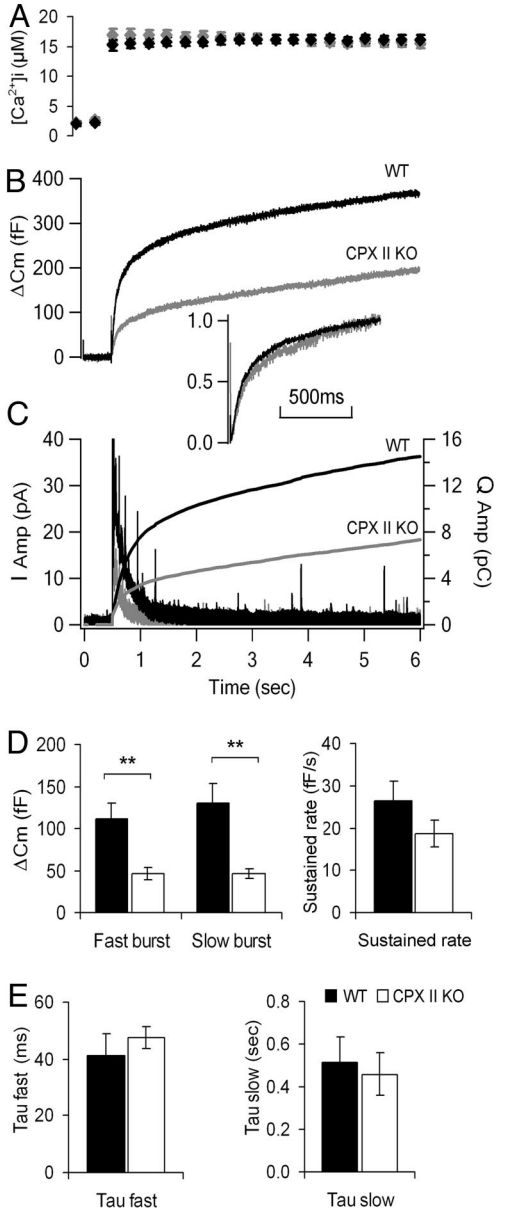

Fig. 4. Exocytosis triggered by photolyzing caged Ca^{2+}. (*A–C*) Averaged $[Ca^{2+}]i$ (*A*), averaged secretion as monitored with membrane capacitance measurements (*B*)m or with amperometry (*C*) from CPX $II^{-/-}$ (gray) and WT (black) cells. (*Inset*) C_m traces were scaled to the same amplitude at 1 s after flash to compare the kinetics of C_m increases. The amperometric traces were also integrated to show the cumulative secretion (*C*). (*D*) Analysis of the size of burst phases and sustained rate of secretion by capacitance measurements. Data were averaged from 13 experiments on 11 WT cells, 4 animals (black, $n = 13$), and from 16 experiments on 11 CPX $II^{-/-}$ cells, 5 animals (white, $n = 16$). **, $P < 0.007$. (*E*) Analysis of the time constants of the fast and slow bursts of secretion (WT, black, $n = 13$; CPX II KO, white, $n = 14$). Data are shown as mean ± SEM.

cells infected by SFV encoding IRES-EGFP (WT+EGFP). Again, Ca^{2+} influx in these two conditions showed no difference, but total secretion was significantly increased upon CPX II overexpression (Fig. 5*G*). The most significant enhancement occurred in the second and third depolarizations and continued to a lesser extent for several more depolarizations (Fig. 5*E*), indicating that the size of the releasable vesicle pools was increased.

Ultrastructure of Wild Type and CPX $II^{-/-}$ Cells. The sustained response in caged Ca^{2+} experiments (Fig. 4*D*) and the late responses in the trains of depolarizations (Fig. 3*E*) were not changed in CPX $II^{-/-}$ cells compared with WT cells, which suggests that the number of docked vesicles is probably not affected by CPXs (docked, unprimed vesicles are the precursor vesicles for resupply of the releasable vesicle pools, after depletion has occurred; a change in the number of precursor vesicles could lead to changes in the net rate of primed vesicle generation). To test this idea further, we performed electron microscopic analysis of the cultured CPX $II^{-/-}$ and CPX $II^{+/+}$ chromaffin cells. We found that the number and spatial distribution of LDCVs—in particular the number of membrane-apposed LDCVs—were indistinguishable between CPX $II^{-/-}$ and CPX $II^{+/+}$ cells (Fig. 6), indicating that vesicle biogenesis and morphological docking are not affected by lack of CPXs.

SNARE-Binding Is Required for the Function of CPX II. The data above show that CPX II increases the size of the releasable vesicle pools. To investigate if this function is related to its ability to bind the SNARE complex, we infected CPX $II^{-/-}$ cells with an SFV vector encoding CPX II with a double mutation K69A/Y70A, which effectively abolishes SNARE binding or CPX II with mutation D29V, which does not affect SNARE binding (Fig. S3) (25). Both mutants were in bicistronic vectors with IRES-EGFP. We then compared the secretion in the transduced cells with CPX $II^{-/-}$ cells transduced with only IRES-EGFP. Our results showed that CPX II D29V rescues the exocytotic burst, whereas CPX II K69A/Y70A does not (Fig. S4), indicating that SNARE binding is needed for complexin function.

Discussion

Our results showing that the fusion kinetics and the dilation of fusion pore are not affected by CPXs were somewhat surprising: A study (21) reported that overexpression of CPX II in bovine chromaffin cells changed the kinetics of fusion pore dilation. That study, however, did not report foot signals, perhaps due to the use of digitonin to permeabilize cell membranes—an approach that has been reported to eliminate foot signals (33). The positive role for vesicle priming is consistent with a role upstream of synaptotagmin 1, and the unaffected fusion kinetics and fusion pore dilation indicate that there is not an obligatory role of CPX downstream of calcium binding to synaptotagmin 1.

Interestingly, we do not see any spontaneous secretion events (spikes) or increase of kiss-and-run events [stand-alone foot, SAF (34)] in CPX $II^{-/-}$ chromaffin cells, when we perform continuous amperometric recordings for up to 20 min (Fig. S5). We also found no change in the vesicle distribution pattern or the vesicle number in the CPX $II^{-/-}$ cells (Fig. 6). These results do not support the simplest form of the recently proposed fusion clamp hypothesis (16, 18–20), where the removal of complexin alone suffices to trigger fusion. However, they do not rule out the possibility that complexin may function together with another protein as a negative clamp. Rather, our data agree with previous work in hippocampal synapses (24) and show that complexin has a net facilitating role during exocytosis at the vesicle priming step, where vesicles are made release-ready. This step seems to precede the possibly calcium-independent association of synaptotagmin with the release machinery (35).

The amino acid residues of the 4 α-helices of the SNARE core complex are aligned in register and in parallel and can be grouped into 16 layers from the N-terminal to the C-terminal, designated layer −7 to layer +8 (36). Studies of mutations at different layers have indicated that the SNARE complexes are partially zipped from N-terminal to C-terminal layer +4 or +5 during vesicle priming (37). Interestingly, crystallographic and NMR studies have shown that the region of CPX-SNARE interaction also extends to layer +4, and, furthermore, binding of CPXs stabilizes the SNARE complex (10). When viewed in this context, our findings are compatible with the idea that CPXs may, through SNARE binding,

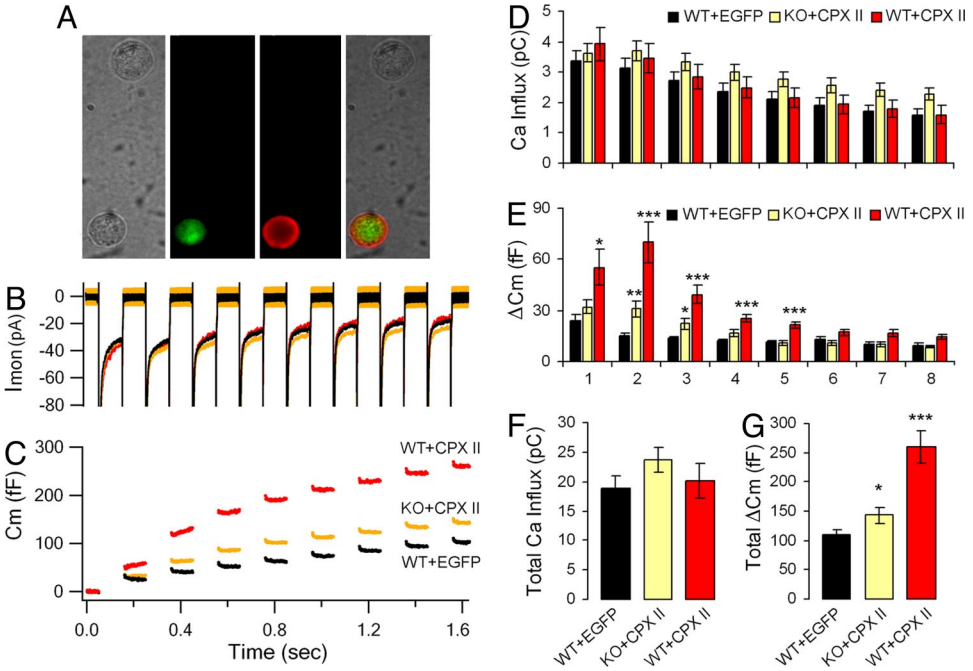

Fig. 5. Secretion of cells transduced with Semliki Forest Virus. (*A*) Immunostaining of CPX II$^{-/-}$ cells rescued by virus-mediated expression of CPX II. The cell (*Lower*) that expresses EGFP (green) can also be labeled by anti-CPX II antibody (red), whereas the cell (*Upper*) that does not express EGFP shows no CPX II labeling. (*B* and *C*) Averaged ionic current recordings (*B*) and capacitance response (*C*). C_m before stimulus was subtracted. (*D*–*G*) Ca^{2+} influxes and ΔC_m for each individual depolarization (*D* and *E*) and summed over all depolarizations (*F* and *G*). Data from WT cells expressing EGFP are in black (WT+EGFP, 38 experiments from 27 cells, 7 animals, $n = 38$), CPX II$^{-/-}$ cells expressing CPX II and EGFP are in orange (KO+CPX II, 27 experiments from 17 cells, 4 animals, $n = 27$), from WT cells overexpressing CPX II and EGFP are in red (WT+CPX II, 14 experiments from 9 cells, 3 animals, $n = 27$). Data are shown as mean ± SEM. *, $P < 0.05$; **, $P < 0.005$; ***, $P < 0.0005$.

stabilize the partially zippered SNARE conformation and the primed vesicle state.

Materials and Methods

Chromaffin Cell Culture and Virus Infection. Mouse breeding was started in the University of Southern California animal facility with CPX II$^{+/-}$ mice. Original CPX mice were generated at the Max Planck Institute of Experimental Medicine, Göttingen, Germany (24). All animal care and experimental treatments were in accordance with USC guidelines for animal care and use. For genotyping, tail biopsies were taken from 1-week-old mice, processed according to standard procedures, and analyzed by PCR. Mice at 8–12 days of age were used for experiments and WT mice from the same litter were used as controls for the CPX II$^{-/-}$ mice in all experiments. Mouse adrenal chromaffin cells were cultured as described in ref. 28. These cells were used at the third and 4th day after culture preparation for all studies reported. For rescue experiments, cells were infected with SFV as described in ref. 38 and cells were used between 15 and 30 h after SFV infection. Recombinant DNA vectors were made with standard molecular biology protocols.

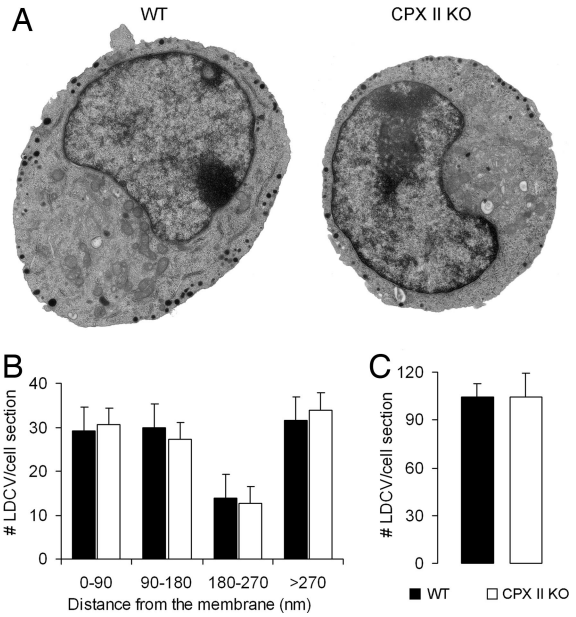

Fig. 6. Ultrastructure of WT and CPX II$^{-/-}$ chromaffin cells. (*A*) Electron micrographs of cultured mouse adrenal chromaffin cells. (*Left*) WT cell. (*Right*) CPX II$^{-/-}$ cell. (*B*) Analysis of the cellular distribution of large dense core vesicles (LDCVs). The distributions were calculated based on the distance from the center of the vesicle to the plasma membrane. The numbers of LDCVs per section in the depicted distance ranges are expressed as mean ± SEM. (*C*) Total number of LDCVs per cell section (mean ± SEM). Data were averaged from 10 WT cells (black, WT), and 13 CPX II$^{-/-}$ cells (white, CPX II KO).

Western Blot Analysis. SDS/PAGE and Western blot analysis were performed as described in ref. 13. Immunoreactive bands were visualized with ECL (GE Healthcare). The antibodies to CPX I/II recognizes both isoforms CPX I and II, but CPX I and CPX II can be distinguished based on their different size. Other antibodies are specific. All primary antibodies were from Synaptic Systems.

Cosedimentation Assays. Recombinant fusion proteins consisting of glutathion-S-transferase (GST) and WT or mutant CPX II were synthesized in *E. coli* using the pGEX-KG expression constructs (39). Recombinant proteins were purified on glutathion-agarose (Sigma) and used, immobilized on the resin, for cosedimentation assays. Crude synaptosomes from rat brain were solubilized at a protein concentration of 2 mg/ml in 150 mM NaCl, 10 mM Hepes (pH 7.4), 1 mM EGTA, 2 mM $MgCl_2$, 1% Triton X-100, 0.2 mM phenylmethylsulfonyl fluoride, 1 μg/ml aprotinin, and 0.5 μg/ml leupeptin (solubilization buffer). After stirring on ice for 10 min, insoluble material was removed by centrifugation (10 min at 346,000 × g_{max} and 4 °C). The equivalent of 3 mg of total protein was then incubated with 50 μg of immobilized GST-fusion protein for 2 h at 4 °C. Beads were then washed 3 times with solubilization buffer, resuspended in SDS/PAGE sample buffer, and analyzed by SDS/PAGE and immunoblotting (40, 41). All primary antibodies were from Synaptic Systems.

Electrophysiological Experiments. Conventional whole cell patch clamp recordings were performed with the EPC-9 amplifier and Pulse software package (HEKA Electronics) (42). A 3.5–4.5 MΩ sylgard-coated pipette was used. Capacitance was measured with the Lindau–Neher technique implemented as the ''sine + dc'' mode of the software lock-in extension of Pulse, in which a 1-kHz, 70-mV peak-to-peak sinusoidal voltage stimulus is superimposed onto a constant holding potential of −80 mV (43). In all of the experiments the isolated chromaffin cells were in an extracellular solution containing 140 mM NaCl, 2.8 mM KCl, 10 mM Hepes, 1 mM $MgCl_2$, 2 mM $CaCl_2$, 2 mM glucose, pH adjusted to 7.2–7.4 and osmolarity adjusted to 290–310. For the experiments where exocytosis was triggered by trains of depolarizations, the pipette solutions contained 10 mM NaCl, 145 mM glutamic acid, 10 mM Hepes, 1 mM $MgCl_2$; titrated with 5 M CsOH

to adjust pH to 7.2–7.4, osmolarity was adjusted to 290–310, ATP/GTP 2 mM/0.3 mM was added before use.

Amperometry. Carbon fiber electrodes were prepared as described in ref. 44 and coupled to a VA-10 amplifier (ALA Scientific Instruments). An 800-mV constant voltage was applied to the electrode relative to Ag/AgCl bath electrode. The amperometry recordings were low-pass filtered at 3 kHz and sampled at 10 kHz. The pipette solution contained: 10 mM NaCl, 50 mM glutamic acid, 1 mM $MgCl_2$, 44 mM $CaCl_2$, 60 mM HEDTA, titrate with 5 M CsOH to pH 7.2–7.4, add ATP/GTP 2 mM/0.3 mM before use. Due to the great variability in the number of amperometric events per cell, we analyzed the data in a way that gave the contribution of each cell the same weight, regardless of the number events for a given cell (45). For each cell and each parameter, we calculated a median value. Then we compared the mean values of the medians of CPX $II^{-/-}$ and CPX $II^{+/+}$ cells.

Photolysis of Caged Ca^{2+}. Caged-Ca^{2+} experiments were performed as described in ref. 46 except the free calcium inside the pipette was adjusted to $\approx$1 μM. A UV flash was generated by a flash lamp (XF-10 xenon flash lamp system, flash bulb XBL-XF/10; Rapp Optoelektronik), and fluorescence excitation was generated by a monochromator (Polychrome V; TILL Photonics). These light sources were coupled into the epifluorescence port of an inverted Axiovert 100 microscope (Zeiss). Calcium dyes were excited at 350/380 nm and the emitted fluorescence was detected with a cascade camera (Cascade 512B; Photometrics) operated by MetaFluor software (Universal Imaging). *In vivo* Ca^{2+} calibration was performed as described in ref. 32. The objectives used were a 40x/1.30 Fluor objective (Zeiss). Both capacitance and amperometry traces were exported to Igor Pro 4.0 (WaveMetrics), and home-written programs were used to perform the analysis. Kinetic analysis of individual capacitance in flash experiments was performed as described in ref. 28. The pipette solution contained 100 mM glutamic acid, 10 mM NaCl, 40 mM Hepes; titrated with CsOH to adjust pH to 7.20 and Osm adjusted to 290–300. 5 mM NP-EGTA, 0.3 mM Furaptra and 0.2 mM Fura-2 were added just before use, and free calcium was adjusted to $\approx$1 μM.

Immunostaining. For cryostat section staining, the dissected adrenal glands were fixed with ice-cold 4% paraformaldehyde in PBS for 2 h and immersed in PBS with 30% sucrose overnight. The glands were sectioned at 12-μm thickness. For cultured cell staining, SFV-infected chromaffin cells were washed in PBS and fixed with ice-cold 4% paraformaldehyde in PBS for 20 min. Cells or gland sections were then washed twice with PBS for 5 min and blocked by 0.2% Triton X-100, 2% goat serum and 2% BSA in PBS for 30 min. Cells or gland sections were incubated overnight at 4 °C with polyclonal rabbit anti-CPX I/II antibody (1:2,000; Synaptic Systems). After washing twice with PBS, cells or gland sections were incubated at room temperature for 1 h with Alexa Fluor 555 goat anti-rabbit IgG (Invitrogen). Cells or gland sections were washed and mounted. The fluorescence was analyzed on an inverted Axiovert 100 microscope with a 40x/1.30 objective (Zeiss).

Electron Microscopy. For ultrastructural analysis, chromaffin cells were plated on collagen-coated coverslips. After 24 h, cells were fixed with 1.5–2.5% glutaraldehyde in 0.1 M phosphate buffer (pH 7.4), incubated on ice for 30 min, and washed thoroughly in phosphate buffer. Cells were postfixed for 1 h in 1% OsO_4 on ice in the dark and further washed. After dehydration through a series of ascending ethanol and propylene oxide, cells were incubated in a 1:1 propylene oxide-Durcupan mix at room temperature and polymerized for 48 h at 60 °C in Durcupan. 50–70 nm ultrathin sections were collected on single-slot grids covered with a Formvar membrane, and contrasted with uranyl acetate and lead citrate solutions. Sections were observed under an LEO 912AB transmission electron microscope (Zeiss). Images were taken with a digital ProScan CCD camera and analyzed with the Analysis 3.2 software (Soft-Imaging-System; Olympus). The distance from the plasma membrane to the center of each LDCV was measured and the number of LDCVs observed was plotted against this distance.

Statistical Analysis. Unless specified, unpaired, 2-tailed Student's *t* test were used to analyze statistical significance. $P < 0.05$ was considered significant.

ACKNOWLEDGMENTS. We thank J. Johnson, W. Xiong, D. Michael, D. Sieburth, S. Hamm-Alvarez, A. Mircheff, L. Zhang and R. Langen for comments. This work was funded by the National Institutes of Health (R.H.C.), the American Heart Association (R.H.C.), the University of Southern California New Faculty Startup Fund (R.H.C.), the Human Frontiers Science Program (N.B. and R.H.C), and the Deutsche Forschungsgemeinschaft (N.B. and J.B.S.).

1. Jahn R, Scheller RH (2006) SNAREs—engines for membrane fusion. *Nat Rev* Mol Cell Biol 7:631–643.
2. Jahn R, Sudhof TC (1999) Membrane fusion and exocytosis. *Annu Rev Biochem* 68:863–911.
3. Chen YA, Scheller RH (2001) SNARE-mediated membrane fusion. *Nat Rev* Mol Cell Biol 2:98–106.
4. Rothman JE (1994) Mechanisms of intracellular protein transport. *Nature* 372:55–63.
5. Weber T, *et al.* (1998) SNAREpins: Minimal machinery for membrane fusion. *Cell* 92:759–772.
6. Sabatini BL, Regehr WG (1999) Timing of synaptic transmission. *Annu Rev Physiol* 61:521–542.
7. MC$_m$ahon HT, Missler M, Li C, Sudhof TC (1995) Complexins: Cytosolic proteins that regulate SNAP receptor function. *Cell* 83:111–119.
8. Pabst S, *et al.* (2002) Rapid and selective binding to the synaptic SNARE complex suggests a modulatory role of complexins in neuroexocytosis. *J Biol Chem* 277:7838–7848.
9. Pabst S, *et al.* (2000) Selective interaction of complexin with the neuronal SNARE complex. Determination of the binding regions. *J Biol Chem* 275:19808–19818.
10. Chen X, *et al.* (2002) Three-dimensional structure of the complexin/SNARE complex. *Neuron* 33:397–409.
11. Ishizuka T, Saisu H, Odani S, Abe T (1995) Synaphin: A protein associated with the docking/fusion complex in presynaptic terminals. *Biochem Biophys Res Commun* 213:1107–1114.
12. Takahashi S, *et al.* (1995) Identification of two highly homologous presynaptic proteins distinctly localized at the dendritic and somatic synapses. *FEBS Lett* 368:455–460.
13. Reim K, *et al.* (2005) Structurally and functionally unique complexins at retinal ribbon synapses. *J Cell Biol* 169:669–680.
14. Ono S, *et al.* (1998) Regulatory roles of complexins in neurotransmitter release from mature presynaptic nerve terminals. *Eur J Neurosci* 10(6):2143–2152.
15. Itakura M, Misawa H, Sekiguchi M, Takahashi S, Takahashi M (1999) Transfection analysis of functional roles of complexin I and II in the exocytosis of two different types of secretory vesicles. *Biochem Biophys Res Commun* 265:691–696.
16. Schaub JR, Lu X, Doneske B, Shin YK, McNew JA (2006) Hemifusion arrest by complexin is relieved by Ca2+-synaptotagmin I. *Nat Struct Mol Biol* 13:748–750.
17. Liu J, Guo T, Wei Y, Liu M, Sui SF (2006) Complexin is able to bind to SNARE core complexes in different assembled states with distinct affinity. *Biochem Biophys Res Commun* 347:413–419.
18. Giraudo CG, Eng WS, Melia TJ, Rothman JE (2006) A clamping mechanism involved in SNARE-dependent exocytosis. *Science* 313:676–680.
19. Tang J, *et al.* (2006) A complexin/synaptotagmin 1 switch controls fast synaptic vesicle exocytosis. *Cell* 126:1175–1187.
20. Huntwork S, Littleton JT (2007) A complexin fusion clamp regulates spontaneous neurotransmitter release and synaptic growth. *Nat Neurosci* 10:1235–1237.
21. Archer DA, Graham ME, Burgoyne RD (2002) Complexin regulates the closure of the fusion pore during regulated vesicle exocytosis. *J Biol Chem* 277:18249–18252.
22. Abderrahmani A, *et al.* (2004) Complexin I regulates glucose-induced secretion in pancreatic beta-cells. *J Cell Sci* 117(Pt 11):2239–2247.
23. Tadokoro S, Nakanishi M, Hirashima N (2005) Complexin II facilitates exocytotic release in mast cells by enhancing Ca^{2+} sensitivity of the fusion process. *J Cell Sci* 118(Pt 10):2239–2246.
24. Reim K, *et al. (2001) Complexins regulate* a late step in Ca2+-dependent neurotransmitter release. *Cell* 104:71–81.
25. Xue M, *et al.* (2007) Distinct domains of complexin I differentially regulate neurotransmitter release. *Nat Struct Mol Biol* 14:949–958.
26. Brose N (2008) For better or for worse: Complexins regulate SNARE function and vesicle fusion. *Traffic* 9:1403–1413.
27. Gil A, *et al.* (2002) Modifications in the C terminus of the synaptosome-associated protein of 25 kDa (SNAP-25) and in the complementary region of synaptobrevin affect the final steps of exocytosis. *J Biol Chem* 277:9904–9910.
28. Sorensen JB, *et al.* (2003) Differential control of the releasable vesicle pools by SNAP-25 splice variants and SNAP-23. *Cell* 114:75–86.
29. Han X, Wang CT, Bai J, Chapman ER, Jackson MB (2004) Transmembrane segments of syntaxin line the fusion pore of Ca^{2+}-triggered exocytosis. *Science* 304:289–292.
30. Borisovska M, *et al.* (2005) v-SNAREs control exocytosis of vesicles from priming to fusion. *EMBO J* 24:2114–2126.
31. Sorensen JB (2004) Formation, stabilisation and fusion of the readily releasable pool of secretory vesicles. *Pflugers Arch* 448:347–362.
32. Voets T (2000) Dissection of three Ca^{2+}-dependent steps leading to secretion in chromaffin cells from mouse adrenal slices. *Neuron* 28:537–545.
33. Grabner CP, Fox AP (2006) Stimulus-dependent alterations in quantal neurotransmitter release. *J Neurophysiol* 96:3082–3087.
34. Wang CT, *et al.* (2003) Different domains of synaptotagmin control the choice between kiss-and-run and full fusion. *Nature* 424:943–947.
35. Nagy G, *et al.* (2006) Different effects on fast exocytosis induced by synaptotagmin 1 and 2 isoforms and abundance but not by phosphorylation. *J Neurosci* 26:632–643.
36. Sutton RB, Fasshauer D, Jahn R, Brunger AT (1998) Crystal structure of a SNARE complex involved in synaptic exocytosis at 2.4 A resolution. *Nature* 395:347–353.
37. Sorensen JB, *et al.* (2006) Sequential N- to C-terminal SNARE complex assembly drives priming and fusion of secretory vesicles. *EMBO J* 25:955–966.
38. Ashery U, *et al.* (2000) Munc13–1 acts as a priming factor for large dense-core vesicles in bovine chromaffin cells. *EMBO J* 19:3586–3596.
39. Guan KL, Dixon JE (1991) Eukaryotic proteins expressed in Escherichia coli: An improved thrombin cleavage and purification procedure of fusion proteins with glutathione S-transferase. *Anal Biochem* 192:262–267.
40. Laemmli UK (1970) Cleavage of structural proteins during the assembly of the head of bacteriophage T4. *Nature* 227:680–685.
41. Towbin H, Staehelin T, Gordon J (1979) Electrophoretic transfer of proteins from polyacrylamide gels to nitrocellulose sheets: Procedure and some applications. *Proc Natl Acad Sci USA* 76:4350–4354.
42. Smith C, Neher E (1997) Multiple forms of endocytosis in bovine adrenal chromaffin cells. *J Cell Biol* 139:885–894.
43. Lindau M, Neher E (1988) Patch-clamp techniques for time-resolved capacitance measurements in single cells. *Pflugers Arch* 411:137–146.
44. Schulte A, Chow RH (1998) Cylindrically Etched Carbon-Fiber Microelectrodes for Low-Noise Amperometric Recording of Cellular Secretion. *Anal Chem* 70:985–990.
45. Colliver TL, Hess EJ, Pothos EN, Sulzer D, Ewing AG (2000) Quantitative and statistical analysis of the shape of amperometric spikes recorded from two populations of cells. *J Neurochem* 74:1086–1097.
46. Nagy G, *et al.* (2002) Protein kinase C-dependent phosphorylation of synaptosome-associated protein of 25 kDa at Ser187 potentiates vesicle recruitment. *J Neurosci* 22:9278–9286.